DOI: 10.61782/fa.2025.0625

FORUM ACUSTICUM EURONOISE 2025

NUMERICAL ANALYSIS OF MINIMUM RESONANCE BANDWIDTHS IN INPUT IMPEDANCES OF HUMAN EAR CANALS

Reinhild Roden[1*] **Matthias Blau**[1,2]

[1] Institut für Hörtechnik und Audiologie, Jade-Hochschule, Oldenburg, Germany.
[2] Cluster of Excellence "Hearing4All".

ABSTRACT

The acoustic input impedance of the human ear canal is a complex function of frequency, reflecting ear canal acoustics and middle and inner ear mechanics. It contains information about the sound pressure at the eardrum and is therefore useful for the individualized equalization of in-ear hearing devices. For clinical applications, it can provide insight into pathological conditions of the ear. To achieve any of the above, it is necessary to determine the ear input impedance with high accuracy. For the validation of impedance measurement system across the entire frequency range up to 16 kHz, for frequency-domain smoothing of measured impedances, as well as for the design of high-frequency couplers, knowledge of the required spectral resolution would be helpful. In this study, minimum relative bandwidths of resonance peaks across the entire frequency range for 41 digitized right ear canal geometries from the IHA database were analyzed, using 3D FEM simulations to determine the input impedance for three different residual ear canal lengths. Results indicate that minimum relative bandwidths decrease from about 0.05 at 5 kHz to around 0.01 at 16 kHz.

Keywords: *hearing acoustics, ear canal, acoustic impedance, FEM simulation*

**Corresponding author*: *reinhild.roden@jade-hs.de.*

1. INTRODUCTION

The input impedance of the ear canal can be used in different applications. A number of studies investigated the viability of employing wideband procedures as a diagnostic tool to ascertain the condition of the middle ear in clinical trials, e.g. [1], [2], [3]. Hence, established medical products integrating these procedures are already available. The main principles of these methods can be found in [4] and [5]. A second class of applications uses the input impedance to estimate the sound pressure at the eardrum, which can potentially be implemented in in-ear hearing systems for individualized equalization aiming at acoustic transparency, e.g. [6]. For the validation of impedance measurement system across the entire frequency range up to 16 kHz, for frequency-domain smoothing of measured impedances, as well as for the design of high-frequency couplers, knowledge of the required spectral resolution would be helpful. This knowledge should be based on the level of spectral detail that would be expected in real ear canal measurements. To this end, the current study analyzes the relative bandwidths of resonances in 3D FEM simulated input impedances of 41 ear canal models from the IHA database [7], [8] for different lengths.

2. METHOD

2.1 Ear canal geometry

The IHA database, containing 3D geometries of torso, head, and complete outer ears with ear canals and eardrums, is being developed. The creation of these geometries was previously described in [7]. For the present contribution, geometry models of the right ear canal of 41 subjects in the database were used. In a first step,

the centerline of each ear canal was determined using the vmtk toolbox [9]. The entrance of the ear canal was then defined as the first plane that is perpendicular to the centerline and intersects the ear canal walls in a way that a closed loop of polygon vertices was created, similar to the method described in [10]. The first and second bends were initially identified through visual inspection and then further refined by locating the nearest local torsion or curvature maximum along the centerline. Of each ear canal, three versions were derived by cuts with planes perpendicular to the centerline, located at the entrance and at the first and second bends, see fig. 1. The eardrum was identified by the following procedure: first, cross-sectional polygons of the medial end of the ear canal were interpolated, and the points with the maximum curvature in the rim region were defined as border points between ear canal wall and the eardrum. Then, the plane with the smallest possible distance to the border points of all cross-sectional polygons was calculated. The tympanic rim was then defined as the intersection of this plane with the 3D geometry. Sometimes, this resulted in unrealistically large eardrums. In these cases, the rotation of the plane was manually adjusted.

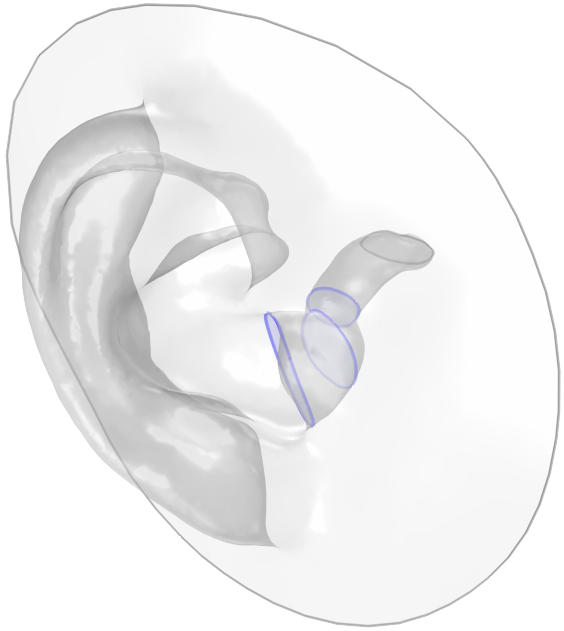

Figure 1. Right outer ear of subject 3 in the IHA database with planes at the entrance, first and second bend (marked blue) and identified eardrum.

2.2 3D FEM simulation

For the three variants of the 41 right ear canals, input impedances Z_{ec} were simulated with COMSOL Multiphysics (6.2) using the 3D finite element method. A normal velocity was assigned to the lateral surface of the residual ear canals as an excitation. Furthermore, the eardrum surface was assigned the impedance of the ear drum and the entire inner ear, according to [11] as implemented in COMSOL. The Helmholtz equation was solved, whereby thermo-viscous effects at the ear canal walls were defined as a boundary condition of the Helmholtz equation, as described in [7] on the basis of [12] and [13], and added to the skin impedance. The values for the skin impedance model are provided by COMSOL as an approximation of the experimental data obtained in [14]. For frequencies up to 20 kHz, sufficient spatial resolution of the sound field was ensured (max. element size of 0.5 mm for boundaries, 1 mm for the volume domain, quadratic (Lagrange) element order). The simulations were run at linearly distributed frequencies between 0.1 and 20 kHz with a frequency resolution of 20 Hz. This corresponds to two hundredths of an octave at 4 kHz, which is the frequency region of first resonances for longer ear canals. The input impedance Z_{ec} resulted from the ratio of the average sound pressure p_{ec} to the volume velocity on the input surface q_{ec},

$$Z_{\mathrm{ec}} = \frac{p_{\mathrm{ec}}}{q_{\mathrm{ec}}}. \tag{1}$$

2.3 Relative bandwidth calculation

All computed input impedances were interpolated to a 1 Hz resolution using a cubic spline interpolation. Subsequently, all resonances with a prominence of at least 3 dB were located. For resonances and anti-resonances, the phase response of the input impedance shows a characteristic rise and a fall, respectively, as exemplarily shown in Fig. 2. All peaks with a corresponding phase zero crossing from +25 to -25 ° were examined. In addition to the harmonics of the first resonance, less prominent side resonances without zero crossing appeared occasionally. These were removed from the analysis. The intersection points of the level of Z_{ec} with a constant line at 3 dB below the respective maximum mark the frequencies of the interval $[f_{-3\mathrm{dB,low}}\ f_{-3\mathrm{dB,high}}]$ for the absolute resonance bandwidth. The frequency f_{mid} was then defined

at the arithmetic mean of that interval. The relative resonance bandwidth was finally calculated as

$$\mathrm{BW_{rel}} = \frac{f_{-3\mathrm{dB,high}} - f_{-3\mathrm{dB,low}}}{f_{\mathrm{mid}}}. \quad (2)$$

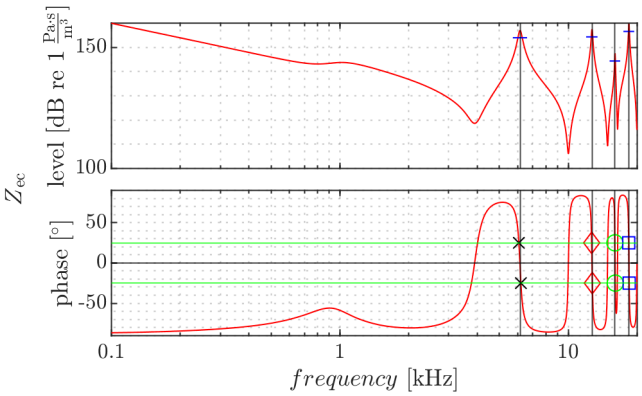

Figure 2. Input impedance for the right ear canal of subject no. 3 cut at the entrance plane.

3. RESULTS

The upper three diagrams in Fig. 3 show the relative resonance bandwidths for ear canals cut at the entrance, the first and the second bend, respectively. Resonances are numbered and sorted by color. For the longest ear canals, up to five resonances were found in the frequency range considered here. The relative resonance bandwidth appears to decay exponentially with logarithmic frequency. The bottom diagram shows all data and a fit using a nonlinear regression model given by

$$\mathrm{BW_{rel}} = 0.26 \cdot \mathrm{e}^{(-0.28\cdot 10^{-3}\cdot \mathrm{f_{mid}/Hz})} + 8.1 \cdot 10^{-3}. \quad (3)$$

This model resulted in an adjusted R^2 of 88.4%.

4. DISCUSSION

Relative resonance bandwidths were calculated for 3D FEM simulations of input impedances on 41 right ear canals of three different lengths. The first resonances occur around 4.5-5 kHz in long ear canals, with relative bandwidths varying between 0.05 and 0.12. Towards higher frequencies, relative bandwidths decay to about 0.01 with decreasing inter-individual variability. A nonlinear model was fitted to this frequency-dependent behavior. The decrease of relative bandwidths with frequency is not surprising, since skin and eardrum are acoustically effective mainly in the mid-frequency range, and their impedances increase at higher frequencies. Keeping in mind that the simulations (a) did not use the higher damping of typical ear canal walls as observed, e.g., in [11] and (b) used an eardrum model that has often been criticized for giving too high impedance values, it appears to be safe to assume a minimum relative bandwidth of 0.01 for the frequency range of human hearing, i.e., up to 16 kHz.

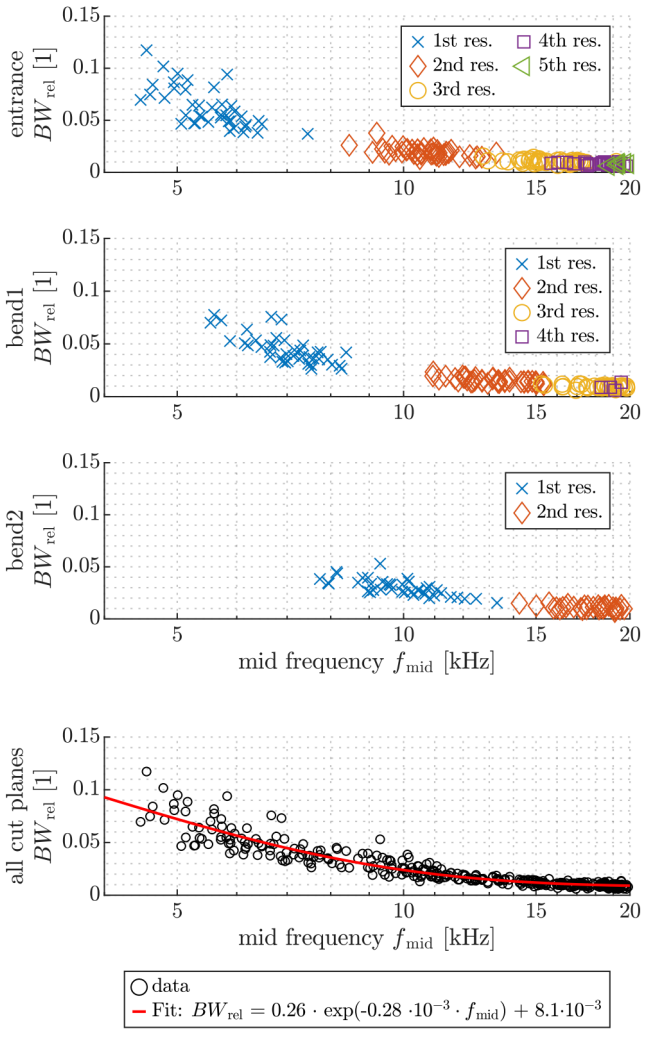

Figure 3. Relative resonance bandwidths of Z_{ec}.

5. CONCLUSION

Relative bandwidths of resonances in the input impedance of human ear canals, computed using 3D FEM simulations with highly conservative assumptions regarding damping effects, are about 0.01 at 16 kHz and larger at lower frequencies. Real ear canals can be expected to exhibit substantially larger relative bandwidths. This result can be used to define the required spectral resolution of impedance measurement systems.

6. ACKNOWLEDGMENTS

This research was partially funded by the Deutsche Forschungsgemeinschaft (DFG, German Research Foundation)—Project ID 352015383—SFB 1330 C1.

7. REFERENCES

[1] Y.-W. Liu, C. A. Sanford, J. C. Ellison, D. F. Fitzpatrick, M. P. Gorga, and D. H. Keefe, "Wideband absorbance tympanometry using pressure sweeps: System development and results on adults with normal hearing," *The Journal of the Acoustical Society of America*, vol. 124, no. 6, pp. 3708–3719, 2008.

[2] C. A. Sanford, D. H. Keefe, Y.-W. Liu, D. Fitzpatrick, R. W. McCreery, D. E. Lewis, and M. P. Gorga, "Sound-conduction effects on dpoae screening outcomes in newborn infants: test performance of wideband acoustic transfer functions and 1-khz tympanometry," *Ear and hearing*, vol. 30, no. 6, p. 635, 2009.

[3] J. J. Rosowski, H. H. Nakajima, M. A. Hamade, L. Mahfoud, G. R. Merchant, C. F. Halpin, and S. N. Merchant, "Ear-canal reflectance, umbo velocity, and tympanometry in normal-hearing adults," *Ear and hearing*, vol. 33, no. 1, pp. 19–34, 2012.

[4] D. H. Keefe, R. Ling, and J. C. Bulen, "Method to measure acoustic impedance and reflection coefficient," *The Journal of the Acoustical Society of America*, vol. 91, no. 1, pp. 470–485, 1992.

[5] S. E. Voss and J. B. Allen, "Measurement of acoustic impedance and reflectance in the human ear canal," *The Journal of the Acoustical Society of America*, vol. 95, no. 1, pp. 372–384, 1994.

[6] S. Vogl and M. Blau, "Individualized prediction of the sound pressure at the eardrum for an earpiece with integrated receivers and microphones," *The Journal of the Acoustical Society of America*, vol. 145, no. 2, pp. 917–930, 2019.

[7] R. Roden and M. Blau, "The iha database of human geometries including torso, head and complete outer ears for acoustic research," in *INTER-NOISE and NOISE-CON Congress and Conference Proceedings*, vol. 261, pp. 4226–4237, Institute of Noise Control Engineering, 2020.

[8] R. Roden and M. Blau, "The iha database of human geometries including torso, head and complete outer ears for acoustic research," 2021.

[9] L. Antiga, *Patient-specific modeling of geometry and blood flow in large arteries*. PhD thesis, Politecnico di Milano, 2002.

[10] A. P. Balouch, K. Bekhazi, H. E. Durkee, R. M. Farrar, M. Sok, D. H. Keefe, A. K. Remenschneider, N. J. Horton, and S. E. Voss, "Measurements of ear-canal geometry from high-resolution ct scans of human adult ears," *Hearing Research*, vol. 434, p. 108782, 2023.

[11] H. Hudde and A. Engel, "Measuring and modeling basic properties of the human middle ear and ear canal. part ii: Ear canal, middle ear cavities, eardrum, and ossicles," *Acta Acustica united with Acustica*, vol. 84, no. 5, pp. 894–913, 1998.

[12] M. Berggren, A. Bernland, and D. Noreland, "Acoustic boundary layers as boundary conditions," *Journal of Computational Physics*, vol. 371, pp. 633–650, 2018.

[13] J. S. Bach and H. Bruus, "Theory of pressure acoustics with viscous boundary layers and streaming in curved elastic cavities," *The Journal of the Acoustical Society of America*, vol. 144, no. 2, pp. 766–784, 2018.

[14] B. Håkansson, P. Carlsson, and A. Tjellström, "The mechanical point impedance of the human head, with and without skin penetration," *The Journal of the Acoustical Society of America*, vol. 80, no. 4, pp. 1065–1075, 1986.